



Characterization of a pressure measuring system for the evaluation of medical devices

Rébecca Bonnaire, Marion Verhaeghe, Jérôme Molimard, Paul Calmels,
Reynald Convert

► To cite this version:

Rébecca Bonnaire, Marion Verhaeghe, Jérôme Molimard, Paul Calmels, Reynald Convert. Characterization of a pressure measuring system for the evaluation of medical devices. Proceedings of the Institution of Mechanical Engineers, Part H: Journal of Engineering in Medicine, 2014, 228 (12), pp.1264-1274. 10.1177/0954411914562871 . hal-01137411

HAL Id: hal-01137411

<https://hal.science/hal-01137411>

Submitted on 30 Mar 2015

HAL is a multi-disciplinary open access archive for the deposit and dissemination of scientific research documents, whether they are published or not. The documents may come from teaching and research institutions in France or abroad, or from public or private research centers.

L'archive ouverte pluridisciplinaire **HAL**, est destinée au dépôt et à la diffusion de documents scientifiques de niveau recherche, publiés ou non, émanant des établissements d'enseignement et de recherche français ou étrangers, des laboratoires publics ou privés.

Original article

Characterization of a pressure measuring system for the evaluation of medical devices

Rébecca Bonnaire^{1,2*}, Marion Verhaeghe³, Jérôme Molimard¹, Paul Calmels⁴ and Reynald
Convert²

¹ LGF, UMR 5307, École Nationale Supérieure des Mines, CIS-EMSE, CNRS, Saint-Etienne, France

² Thuasne, Levallois-Perret, France

³ Université de Technologie de Compiègne, Compiègne, France

⁴ Université de Lyon, Laboratoire de Physiologie de l'Exercice, F-42023, Saint-Etienne, France

*** Corresponding author :**

Rébecca Bonnaire, LGF, UMR 5307, Ecole Nationale Supérieure des Mines de Saint-Etienne, CS 62362,
F-42023 Saint-Etienne cedex 2, France

Email : bonnaire@emse.fr

Abstract

The purpose of this study is to evaluate the possible use of four “FSA” thin and flexible resistive pressure mapping systems, designed by Vista Medical (Winnipeg, Manitoba, Canada), for the measurement of interface pressure exerted by lumbar belts onto the trunk. These sensors were originally designed for the measurement of low pressure applied by medical devices on the skin.

Two types of tests were performed: standard metrology tests such as linearity, hysteresis, repeatability, reproducibility and drift, and specific tests for this application such as curvature, surface condition and mapping system superposition.

The linear regression coefficient is between 0.86 and 0.98; hysteresis is between 6.29% and 9.41%. Measurements are repeatable. The location, time and operator, measurement surface condition and mapping system superposition have a statistically significant influence on the results. A stable measure is verified over the period defined in the calibration procedure, but unacceptable drift is observed afterward. The measurement stays suitable on a curved surface for an applied pressure above 50mmHg.

To conclude, the sensor has acceptable linearity, hysteresis and repeatability. Calibration must be adapted to avoid drift. Moreover, when comparing different measurements with this sensor the location, the time, the operator and the measurement surface condition should not change; the mapping system must not be superimposed.

Keywords

Pressure measurement, pressure mapping system, medical device, mechanical characterization, metrology

Introduction

Low back pain is a major public health problem in developed countries. In France, prevalence of low back pain is higher than 50% [1]. Because of health care costs and sick leave [1-2], low back pain has adverse consequences on both the social and economic level. Many treatments have been proposed. However, no guidelines are proposed to practitioners, particularly for chronic evolution. Treatment propositions and success depend on the patient comportment, on the aetiology and/or mechanical causes of low back pain, on the evolution along the time and also on the physician's opinions. Lumbar belts are frequently proposed to treat low back pain. Several clinical trials have shown their clinical effectiveness [3-4]. Nevertheless, both the mechanical and the physiological effects of lumbar belts remain unclear.

It is assumed that the main mechanical effect of lumbar belts is the pressure applied on the trunk; therefore it has been decided to investigate experimentally this pressure. In the medical field, pressure measurement is already used to evaluate devices employed to prevent bedsores [5-11], to measure the interface pressure of compression stockings, compression bandages [12-18] and rigid orthosis [19-20]. Using pressure measurement to mechanically characterize lumbar belts can be considered as new approach.

Four types of interface pressure sensors exist: pneumatic (Example: PicoPress[®], St Neots Cambridgeshire, United Kingdom), electro-pneumatic (Example: Salzmann[®], St. Gallen, Switzerland), resistive (Example: Tekscan[®], Boston MA, USA) or capacitive (Example: X-Sensor[®], Calgary Alberta, Canada or Novel[®], Munich Germany) sensors. Resistive or capacitive sensors may be assembled into a structure that enables the pressure to be measured at several points simultaneously; this structure is often called a pressure mapping system.

In this study, four identical FSA[®] pressure mapping systems were chosen and purchased (Vista Medical[®], Winnipeg Manitoba, Canada). They are composed of resistive sensors, based on the piezoresistive

properties of some materials. The resistivity of piezoresistive materials varies according to the forces exerted on this material. Resistivity is proportional to the electrical resistance which is converted into voltage. After calibration, measurement of voltage enables the interface pressure to be measured [21]. These pressure mapping systems were chosen because they are thin and compliant, free from error of measurement on curved surfaces, sensitive in detecting a range of pressure as low as 0-100mmHg (0-13.3kPa), in accordance to in-vivo studies (free from temperature or moisture effects, dynamic range ≥ 10 Hz) and give indications of pressure gradients in a context of spatial variations of support stiffness and shape [22-24]. Compared to the capacitive sensors, resistive sensors have a lower drift and are less expensive [25-26].

Aim of this study is to evaluate these four identical pressure mapping systems, particularly in challenging applications such as lumbar belts. This evaluation is performed by two types of tests:

- classical tests of metrology such as linearity, hysteresis, repeatability, reproducibility and drift,
- specific test for the application developed in this study, such as curvature, surface condition and mapping system superposition.

The goal of classical tests is to determine the proper functioning of sensors in their general use. The goal of specific tests is to characterize the pressure sensors in case of interface pressure measurement between the trunk and the lumbar belt. Actually, in this specific type of measurement, surfaces are soft and curved. Moreover, the four pressure mapping systems may be partially superimposed during the measurement.

Methods

The FSA pressure mapping systems

Four mapping systems are needed to measure the interface pressure all around the trunk. In this study, the mapping systems will be tested all together and no comparison between them will be done. Pressure mapping systems are composed of 12 by 32 piezoresistive sensors. Each sensor is a square with sides measuring 7.9mm, separated by 4.2mm. The active area is 382 by 142mm. The total size of the mapping system is 482 by 242mm. Sensor calibration is performed with the pressure range from 0 to 100mmHg. During calibration, 50mmHg is measured for 60 seconds to compensate the drift effect. The FSA pressure mapping system is illustrated in Figure 1. The pressure mapping systems are denoted below A, B, C and D.

Classical tests of metrology [27]

Linearity test. For the linearity test, seven cylindrical steel weights were designed to apply pressure between 6 and 96mmHg on one sensor. Weights were randomly applied in sensors 1, 2 and 3 (see Figure 1). Thirty measurements were carried out for each sensor. The linear regression coefficient R^2 between applied and measured pressures, the dispersion and the standard deviation s_p were calculated. The linear regression coefficient R^2 is defined by the following formula:

$$R^2 = \frac{cov(P, P_i)^2}{var(P)var(P_i)} \quad (1)$$

with P , the measured pressure value in mmHg and P_i , the applied pressure value in mmHg.

The dispersion is defined as the difference between the maximum and the minimum pressure measured for each applied pressure. The standard deviation s_p of the measured pressure is defined by the following formula:

$$s_p = \sqrt{\frac{1}{(n-1)} \sum_{i=1}^n (P_i - \bar{P})^2} \quad (2)$$

with n, the size of the measured sample and P, the measured pressure value for each applied pressure in mmHg.

Hysteresis test. Two types of hysteresis tests were performed: an hysteresis test in only one sensor and an hysteresis test in all sensors at the same time of the mapping system.

For the first test, the same weights as for the linearity test, were increasingly and decreasingly applied on eight sensors. The position of these sensors is represented in Figure 1. For the second test, pressure mapping was placed on an air pocket and introduced between two wooden planks. Figure 2 illustrates this experimental device. The air pocket was inflated to apply increasing then decreasing pressure between 10 and 100mmHg to the mapping system.

Hysteresis is defined by the following formula:

$$E_h(\%) = \frac{|y_d(x_i) - y_m(x_i)|}{x_i} * 100 \quad (3)$$

with x_i , the discrete values of applied pressure in mmHg, y_m the measured pressure value during the increasing phase corresponding to a given x_i in mmHg, and y_d the measured pressure value during the decreasing phase corresponding to a given x_i in mmHg.

Repeatability test. The repeatability of experiments was assessed by performing the first hysteresis test three times. Repetitions were compared by statistical analysis as explained in paragraph 2.4.

Reproducibility test. The reproducibility of time, location and operators was tested. The first hysteresis test was performed in two different rooms, by two different operators and at two different times separated by two months.

A specific design of experiments was used to evaluation reproducibility (Table 1). In this design of experiments, there are four independent factors: location, time, operators and weight applied to the mapping system. The interactions between each factor are considered. The selected design of experiments is factorial and follows this polynomial model:

$$P = \sum_i \beta_i x_i + \sum_{ij} \beta_{ij} x_i x_j \quad (4)$$

with P, the measured pressure (mmHg), β_i or β_{ij} , the polynomial coefficients and x_i or x_j , the input factor of the design of experiments.

Drift test. To determine if the pressure recorded changes over time, four weights corresponding to 26, 40, 52 and 80mmHg applied pressure were left on 1, 2, 3, 4, 5 and 6 sensors (see Figure 1) for a duration higher than that of the calibration to drift (30 minutes).

For each case, the range of stored drift, as defined by the minimum and maximum pressures measured during the testing, was determined. The relative pressure variation was expressed by the following formula:

$$\Delta P_r = \frac{|P_m - P_a|}{P_a} \quad (5)$$

with ΔP_r the relative pressure variation, P_m the measured pressure and P_a the applied pressure.

Tests specific to the application

Curvature test. An experimental setup was developed to characterize the impact of measurement on curved surfaces. This experimental setup consists in a support on which it is possible to place cylinders of different radii. Radii used in this study were 60, 80, 100 and 125mm. Pressure mapping systems were placed on the cylinder. Pressure was applied on one single line of sensors using a 15mm band, at the end of which weights were hung on. This experimental setup is illustrated in Figure 3. Three lines were tested

for one mapping system. As results were similar for these three lines, just one line was tested for the other three pressure mapping systems. Six or seven different pressures were applied per cylinder, per line and per pressure mapping system.

For each applied pressure, cylinder and pressure mapping system, normalized pressure was calculated according to the following formula:

$$P_n = \frac{P_m}{P_a} \quad (6)$$

with P_n the normalized pressure, P_m the measured pressure and P_a the applied pressure.

Surface condition test. The possible application of this system is to measure the interface pressure applied by lumbar belts. Usually these belts are worn over garments (tee shirt, shirts, etc.). The surface condition of the measured zone is important. Two different surface conditions have been tested. Evaluation of the effect of the surface condition was done in two stages.

Firstly, a hysteresis test was performed with only one sensor and seven different medical fabrics placed between the table and the mapping system. For two of the tested fabrics, the pressure decrease was more than 50%. Therefore, these two fabrics were not considered for the statistical analysis. For the other five fabrics, two statistical analyses were performed. The first one was used to compare results with and without fabric between the pressure mapping system and the table. The second one was used to determine if results are different depending on fabrics inserted between the table and the pressure mapping system.

Secondly, the hysteresis test was conducted with only one sensor with weights surrounded by silicone and with froth positioned between the table and the mapping system. Statistical analysis was done to determine if there are statistical significant differences between results for this test and for the first test of hysteresis (test in one sensor). The linear regression coefficient was calculated thanks to equation 1.

Mapping system superposition test. To determine the impact of two superimposed pressure mapping systems on the results, the first hysteresis test (test in one sensor) was performed in three sensors stacking two mapping systems.

Statistical analysis was performed to determine if there are statistical significant differences between results for the pressure mapping system “from above” and the pressure mapping system “from the bottom”. Absolute differences between measured pressures with or without superposition were calculated for each pressure mapping system.

Statistical analysis

Statistical analysis was used to determine differences between two or more than two distributions. Depending on the number of data sets to compare, two types of statistical approach were used. A Jarque-Bera test was used to check whether or not data matched normal distribution.

To compare two sets of data, a Student t-test was used if they were distributed following a normal distribution, and a Wilcoxon signed ranks if not. The statistical analysis of two distributions was used for mapping system superposition and surface condition tests. Student t-test was also used for the linearity test to determine if the linear regression curve’s slope is zero.

To compare more than two sets of data, an ANOVA was used if they were all distributed following a normal distribution, and a Kruskal-Wallis test if not. If needed, the post-hoc test of Tukey was used to find which of the data sets were different. The statistical analysis of more than two distributions was used for repeatability and surface condition tests.

All the statistical tests were performed with a risk α to be equal or smaller than 5%.

Results

Classical tests of metrology

Linearity. Linear regression coefficients and p-value of the Student's test on slope=0 are given in Table 2. The results are illustrated for one sensor of one mapping system in Figure 4. The linear regression coefficient R^2 is between 0.86 and 0.98 depending on the sensor and the mapping system. The maximum dispersion and the maximum standard deviation to the measured pressure are 18.9 and 9.60mmHg respectively. Table 3 shows the results of maximum dispersion and maximum standard deviation for sensors with the best and the worst linearity.

Hysteresis. All results are given in Table 4. For the first test of hysteresis (test in only one sensor), hysteresis is between 0.228% and 27.9%. An example of results for the second hysteresis test (test in all sensors of a pressure mapping system) is given in Figure 5. For this test of hysteresis, the hysteresis is between 6.29% and 9.41%. All results are given in Table 5.

Repeatability. The Kruskal-Wallis test shows no difference (p-value = 0.88). Measurements are repeatable.

Reproducibility. Table 6 indicates the polynomial coefficient of the experimental design model and probability that the factor x_i has at least a 95% chance of not significantly affecting the response to pressure of the sensors. x_i can be time, space, operators, weight or interactions factors. The biggest polynomial coefficient corresponds to the weight influence and the smaller corresponds to the time influence. Location, weight, time coupling with operators and time coupling with location have statistical influence to the measured pressure.

Drift. No significant drift was observable during the first 60 seconds, i.e. the calibration time for drift. After that period, three types of drift are obtained: measured pressure increases during the first few minutes and becomes stable, measured pressure decreases during the first few minutes and becomes stable and measured pressure is stable over time. Figure 6 represents these three typical results. For all sensors, measured pressure becomes stable and reaches its nominal value after 800 seconds.

Tests specific to the application

Curvature. Figure 7 shows results for the mapping pressure system A. The results depend on the applied pressure. When the applied pressure is less than 50mmHg, the measured pressure is lower than the applied pressure. Nevertheless, when the applied pressure is more than 50mmHg, the difference between the applied pressure and the measured pressure is minor.

Surface condition. The probabilities of there being at least a 95% chance that results with and without fabric between the pressure mapping system and the table are different for the five tested fabrics are given in Table 7. All fabrics have a statistically significant influence on the results.

The Kruskal-Wallis test is significant ($p\text{-value} < 0.001$). The five fabrics are statistically significantly different. Only measured pressure for fabrics 1 and 2, 3 and 4, and 3 and 5 do not have a statistically significant difference.

For the second surface condition test, the linear regression coefficient R^2 is between 0.95 and 0.99, depending on the sensor and the mapping system. Hysteresis is between 4.2% and 15%. For the third surface condition test, the linear regression coefficient R^2 is between 0.92 and 0.98. Detailed results for the second and third tests are presented in Table 8.

Mapping system superposition. Mapping system superposition results consist of two distributions: measured pressure for the mapping systems “from above” and for the mapping systems “from the bottom”.

Results for the test of Wilcoxon signed rank, to compare results for the mapping systems “from above” and “from the bottom”, are given in Table 9. Table 10 indicates absolute differences between measured pressures with or without superposition for each pressure mapping system.

Discussion

In this study, four identical pressure mapping systems were evaluated in term of linearity, hysteresis, reproducibility and drift. Some other evaluations demonstrated the efficacy of the pressure mapping systems in the specific application of lumbar belts characterization. According to the results, pressure mapping systems are suitable for this application.

We found that linearity is acceptable according to the linear regression coefficient R^2 which is always greater than 0.85. Pressure measured with sensors is always underestimated. The maximum deviation is 15.4mmHg. The hysteresis of the pressure mapping system depends on sensors. On the whole, hysteresis is low between 6.29% and 9.41%. Measurements are repeatable. The reproducibility test shows the influence of experimental location, time and operator; the most influencing parameter is the location. According to the drift test, the value remains stable if the measuring time remains lower than the drift calibration time, but dramatically changes afterward.

Thanks to our tests specific to the application, it is possible to conclude that curvature test results depend on the applied pressure. For applied pressure higher than 50mmHg, measurement is the same as on a flat surface. Nevertheless, for applied pressure less than 50mmHg, the measured pressure is lower than the applied pressure. This can be explained by the experimental device. It is supposed that the band sticks on the cylinder when the applied pressure is too low and the pressure estimation from Laplace's law is not valid any more. Thus, no conclusions to the impact of curvature for low measured pressure can be drawn from these results.

We also proved that the surface measurement has a significant influence on the measured pressure. However, there is no change in hysteresis and linearity when pressure is measured between two soft surfaces. In this case, hysteresis is between 4.2% and 15% and the linear regression coefficient is between

0.92 and 0.98. Last, the superposition of two pressure mapping systems can have a significant influence on the measurement.

Comparison of the FSA pressure mapping system to the other resistive pressure mapping systems

Metrological results of other sensors have been collected from the literature: Flexiforce[®] [22], F-Socket[®] [25] and F-Scan[®] [21] sensors from Tekscan[®], Rincoe's sensor [25] and Lück sensor [29]. Measurement error and hysteresis are summarized in Table 11. For accuracy, FSA sensor is identical (Flexiforce[®], F-Socket[®]) or even better (Rincoe, Lück, F-Scan[®]) than other pressure mapping systems. For hysteresis, performances of other resistive sensors are identical (Flexiforce[®]) or lower (F-Socket[®], Rincoe) than the FSA[®] sensor. Measurement is repeatable for all resistive sensors [22-23]. Other resistive sensors drift as well: Flexiforce sensors' measurements increase or decrease with time [22] [26]; Rincoe SFS and F-Socket[®] from Tekscan[®] sensors' measurements increase with time [21] [25]. The increase or decrease of the measurement varies from 7.4% to 11.9% in twenty minutes [25]. According to the literature, the curvature of the measurement surface has an influence, for other resistive sensors than FSA[®] sensor on the measurement regardless of the pressure range. The sensitivity of the Tekscan[®]'s Flexiforce[®] sensor is modified with radius of curvature [22]. For Rincoe SFS and F-Socket[®] sensors from Tekscan[®], accuracy decreases, drift error increases and hysteresis can increase or decrease with radius of curvature [25]. No data was found to compare the FSA[®] sensor with other resistive sensors in term of reproducibility, surface condition and superposition of two pressure mapping system.

Comparison of the FSA pressure mapping system to the capacitive pressure mapping system

It is also possible, according to data from the literature, to compare the FSA[®] sensors with other types of pressure mapping systems for measuring interface pressure: the X-Sensor[®] capacitive pressure mapping

system [21, 28, 29] and Novel[®] distributed sensors [23]. For linearity, the X-Sensor[®] is linear [28] and measures 75.1% of the applied pressure [21]. The capacitive sensor may demonstrate a worse performance than FSA[®]. The maximum measurement error for X-Sensor[®] is 65% of applied pressure or 27mmHg [29]. Novel[®]'s sensor demonstrates a superior performance: its linear coefficient is 0.997 and the measurement error is less than 1mmHg [23]. But capacitive sensors have a greater hysteresis than resistive sensors. For example, the X-Sensor[®] hysteresis is 14% [28]. Measurement with capacitive sensors is repeatable [23-24]. According to the drift test, measured pressure with capacitive sensors increases with time [21] [26]. Concerning the surface condition, capacitive sensors, X-Sensor[®] and Novel[®], allow better or worse measurement on soft surfaces depending on the thickness of these surfaces [28]. No data was found to compare the FSA[®] sensor with capacitive sensors in terms of reproducibility, curvature and superposition of two pressure mapping systems.

Considerations on the use of FSA[®] pressure mapping system for the clinical study of lumbar belt

Based on these results, it is necessary to take into account some points to develop the experimental protocol. First, to be accurate, measurement must be done in the same place and preferably by the same operator and in short time frame. It's easy to perform measurement in the same place, but it's more difficult, in a clinical field, to respect the two other points, because measurements is often done by more than one experimenter and it's difficult to find enough subjects in a short time frame. However, these two parameters have influence on the results with coupled parameters. Secondly, drift result shows the importance in the choice of the drift calibration period, drift being uncontrolled if the measuring time is higher. Actually, during calibration, the central value of the calibration interval is measured for a flexible period. Pressure mapping system was calibrated in this study with a flexible period of 60 seconds, but the period can be increased to more than 800 seconds to avoid drift. This solution permits to perform dynamic measurements. Third, improving the curvature test is necessary before beginning the clinical

study to ensure that the measurement of low pressure will be accurate on curved surfaces. Fourthly, surface condition having an influence on the results, pressure measurements will be done between lumbar belts and a tee-shirt of the same composition for all experiments and all subjects. Whatever the surface condition, pressure measurement remains accurate in term of linearity and hysteresis. Finally, the pressure mapping systems will be used to never overlap while covering the whole trunk. To overcome the difficulty of this condition, measures will be taken side by side. All these conditions allow a suitable measurement of pressure and to compare pressure applied by lumbar belt in term of lumbar belt's types and patient's morphology.

To conclude, the FSA[®] sensor performance can be considered as better than other resistive sensors and demonstrates an identical performance to the capacitive sensor X-Sensor[®] with lower hysteresis. Nevertheless, the capacitive sensor Novel demonstrates a better performance than the FSA[®] sensor, but has a higher drift effect. FSA[®] sensors can be a good choice for the future clinical study developed to measure the static pressure applied by the lumbar belt on the trunk, because this study will be done in the same place, in a short time frame, with the same operator, with no overlapped mapping system and between same types of surface. Indeed, the procedure described earlier with FSA[®] pressure mapping system still lacks of robustness for a routine clinical practice to evaluate pressure applied by lumbar belts prescribed to the low back pain patients.

Conclusion

In this study, four FSA[®] pressure mapping systems were characterized in term of linearity, hysteresis, repeatability, reproducibility, drift, curvature, surface condition and mapping system superposition. It was found that these pressure mapping systems are suitable for our application: pressure measurement between two soft surfaces, lumbar belt and the human trunk. Linearity, accuracy and hysteresis are

adequate. Measurement is repeatable and suitable on a flat surface. The curvature of the surface measurement has no significant impact on the measured pressure.

However, it is necessary to take into account some recommendations before performing measurements with this FSA[®] sensor. To compare the results of different experiments, measurement must be performed in the same place, over a short timeframe, with the same operator. Calibration must be adapted to prevent sensor drift. The measurements shall concern the same type of surface. Moreover, it is important to avoid overlap of pressure mapping systems.

Further study is needed to evaluate the performance of the sensor on a curved surface when applied pressure is lower than 50mmHg and also how the sensor behaves when temperature and humidity change.

Acknowledgements

The authors would like to thank Mr. Poirier for his assistance with this work.

Conflict of interest

There is no conflict of interest in this study.

Funding:

This research received no specific grant from any funding agency in the public, commercial, or not-for-profit sectors.

References

1. Fassier JB. [Prevalence, costs and societal issues of low back pain]. *Rev Rhum* 2011; 78(sup.2): S38-S41. French

2. Leclerc A, Gourmelen J, Chastang JF, Plouvier S, Niedhammer I, Lanoë JL. Level of education and back pain in France: the role of demographic, lifestyle and physical work factors. *Int Arch Occup Environ Health* 2009; 82(5): 643-652.
3. Calmels P, Galtier B, Carzon JG, Poinsignon JP, Vautravers P, Delarque A. Etude de l'effet antalgique et fonctionnel du port d'une orthèse lombaire souple dans la lombalgie aiguë. *Annales de Réadaptation et de Médecine Physique* 1999; 42(6): 333-340.
4. Calmels P, Queneau P, Hamonet C, Le Pen C, Maurel F, Lerouvreur C, Thoumie P. Effectiveness of a lumbar belt in subacute low back pain: an open, multicentric and randomized clinical study. *Spine* 2009; 34(3): 215-220.
5. Vaisbuch N, Meyer S, Weiss PL. Effect of seated posture on interface pressure in children who are able-bodied and who have myelomeningocele. *Disabil Rehabil* 2000; 22(17): 749-755.
6. Fenety PA, Putnam C, Walker JM. In-chair movement: validity, reliability and implications for measuring sitting discomfort. *Appl Ergon* 2000; 31(4): 383-393.
7. Shelton F, Lott JW. Conducting and interpreting interface pressure evaluations of clinical support surfaces. *Ger Nursing* 2003; 24(4): 222-227.
8. Tam EW, Mak AF, Lam WN, Evans JH, Chow YY. Pelvic movement and interface pressure distribution during manual wheelchair propulsion. *Arch Phys Med Rehabil* 2003; 84(10): 1466-1472.
9. Reenalda J, van Geffen P, Nederhand M, Jannink M, IJzerman M, Rietman H. Analysis of healthy sitting behavior: interface pressure distribution and subcutaneous tissue oxygenation. *J Rehabil Res Dev* 2009; 46(5): 577-586.

371 10. Rithalia SV, Heath GH, Gonsalkorale M. Assessment of alternating-pressure air mattresses using a
372 time-based pressure threshold technique and continuous measurements of transcutaneous gases. *J Tissue*
373 *Viability* 2000; 10(1): 13-20.

374 11. Hamanami K, Tokuhira A, Inoue H. Finding the optimal setting of inflated air pressure for a multi-
375 cell air cushion for wheelchair patients with spinal cord injury. *Acta Med. Okayama* 2004; 58(1): 37-44.

376 12. Partsch H, Partsch B, Braun W. Interface pressure and stiffness of ready made compression stockings:
377 comparison of in vivo and in vitro measurements. *J Vasc Surg* 2006; 44(4): 809-814.

378 13. Hafner J, Lüthi W, Hänssle H, Kammerlander G, Burg G. Instruction of compression therapy by
379 means of interface pressure measurement. *Dermatol Surg* 2000; 26(5): 481-486.

380 14. Damstra RJ, Brouwer ER, Partsch H. Controlled, comparative study of relation between volume
381 changes and interface pressure under short-stretch bandages in leg lymphedema patients. *Dermatol Surg*
382 2008; 34(6): 773-778.

383 15. Damstra RJ, Partsch H. Compression therapy in breast cancer-related lymphedema: A randomized,
384 controlled comparative study of relation between volume and interface pressure changes. *J Vasc Surg*
385 2009; 49(5): 1256-1263.

386 16. Dumbleton T, Buis AWP, McFadyen A, McHugh BF, McKay G, Murray KD, Sexton S. Dynamic
387 interface pressure distributions of two transtibial prosthetic socket concepts. *J Rehabil Res Dev* 2009;
388 46(3): 405-415.

389 17. Candy LHY, Cecilia LTWP, Ping ZY. Effect of different pressure magnitudes on hypertrophic scar in
390 a Chinese population. *Burns* 2010; 36(8): 1234-1241.

18. Reich-Schupke S, Gahr M, Altmeyer P, Stücker M. Resting pressure exerted by round knitted moderate-compression stockings on the lower leg in clinical practice--results of an experimental study. *Dermatol Surg* 2009; 35(12): 1989-1997.
19. van den Hout JAAM, van Rhijn LW, van den Munckhof RJH, van Ooy A. Interface corrective force measurements in Boston brace treatment. *Eur Spine J* 2002; 11(4): 332-335.
20. Aubin CE, Labelle H, Cheriet F, Villemure I, Mathieu PA, Dansereau J. Évaluation tridimensionnelle et optimisation du traitement orthopédique de la scoliose idiopathique adolescente. *MS. Médecine Sciences* 2007; 23(11): 904-909.
21. Fergenbaum MA, Hadcock L, Stevenson JM, Bryant JT, Morin E, Reid SA. Development of a dynamic biomechanical model for load carriage: Phase 4, Part C2: Assessment of Pressure Measurement Systems on Flat Surfaces for the Dynamic Biomechanical Model of Human Load Carriage. *Contract Report*, Queen's University, Kingston, Ontario, Canada. 2005; 33p.
22. Ferguson-Pell M, Hagisawa S, Bain D. Evaluation of a sensor for low interface pressure applications. *Med Eng Phys* 2000; 22(9): 657-663.
23. Lai CHY, Li-Tsang CWP. Validation of the Pliance X System in measuring interface pressure generated by pressure garment. *Burns* 2009; 35(6): 845-851.
24. Chiang CC, Lin CCK, Ju MS. An implantable capacitive pressure sensor for biomedical applications. *Sens Actuators A Phys* 2007; 134(2): 382-388.
25. Polliack AA, Sieh RC, Craig DD, Landsberger S, McNeil DR, Ayyappa E. Scientific validation of two commercial pressure sensor systems for prosthetic socket fit. *Prosthet Orthot Int* 2000; 24(1): 63-73.

- 411 26. Wheeler JW, Dabling JG, Chinn D, Turner T, Filatov A, Anderson L, Rohrer B. MEMS-based bubble
412 pressure sensor for prosthetic socket interface pressure measurement. *Conf Proc IEEE Eng Med Biol Soc*
413 2011; 2925-2928.
- 414 27. BIPM, IEC, IFCC, ILAC, IUPAC, IUPAP, ISO, OIML. The international vocabulary of metrology—
415 basic and general concepts and associated terms (VIM), 3rd edn. *JCGM* 200:2012.
- 416 28. Hochmann D, Diesing P, Boenick U. Evaluierung der Messmethoden zur Bewertung des
417 Therapeutischen nutzens von Antidekubitus-Systemen. *Biomed Tech* 2002;47(suppl 1 pt 2):816-819.
- 418 29. Völker HU, Rölker N, Willy C. Auflagedruckmessung in der Dekubitusbehandlung. *Anaesthesist*
419 2006; 55(2): 142-147.
- 420

421 **Table captions**

422 Table 1. Design of experiments to test the reproducibility of time, place and operators

423 Table 2. Results of linearity: linear regression coefficient

424 Table 3. Results of linearity: dispersion and standard deviation for sensor 1 and mapping system C

425 Table 4: Results of hysteresis: test in only one sensor per mapping system

426 Table 5. Results of hysteresis: test in all sensors per mapping system

427 Table 6. Results of the design of experiments for reproducibility. t: time, o: operators, l: location, w:

428 weight

429 Table 7. Results of surface condition: 95% probability of a significant difference between measured

430 pressure with and without fabric between the pressure mapping system and the table are different for the

431 five tested fabrics

432 Table 8. Results of surface condition: linear regression coefficient for the second and third surface

433 condition tests

434 Table 9. Results of mapping system superposition: 95% probability of a significant difference between

435 the mapping system “from above” and “from the bottom”

436 Table 10. Results of mapping system superposition: absolute differences between measured pressures

437 with or without superposition for each pressure mapping system

438

Figure captions

Figure 1. FSA Pressure mapping system

Figure 2. Experimental device for the second hysteresis test

Figure 3. Experimental device for curvature test

Figure 4. Results of linearity: measured pressure depending on applied pressure for the sensor 1 of the pressure mapping system A

Figure 5: Results of the second hysteresis test (test in all sensors of a pressure mapping system): mean measured pressure depending on applied pressure for mapping system A

Figure 6. Results of drift: a. drift for 26mmHg applied pressure for mapping system A in the sensor 1, b. drift for 40mmHg applied pressure for mapping system C in the sensor 1, c. drift for 26mmHg applied pressure for mapping system D in the sensor 3

Figure 7. Results of curvature: normalized measured pressure depending on applied pressure and radius of cylinders R_c for mapping system A

452 Table 1. Design of experiments to test the reproducibility of time, place and operators

| Experiments | Time -1: t0 +1: t0 + 2 months | Operators -1: operator A +1: operator B | Location -1: place A +1: place B | Weight -1: 53mmHg +1: 79mmHg |
|-------------|-------------------------------------|---|--|------------------------------------|
| 1 | -1 | -1 | -1 | -1 |
| 2 | +1 | -1 | -1 | -1 |
| 3 | -1 | +1 | -1 | -1 |
| 4 | +1 | +1 | -1 | -1 |
| 5 | -1 | -1 | +1 | -1 |
| 6 | +1 | -1 | +1 | -1 |
| 7 | -1 | +1 | +1 | -1 |
| 8 | +1 | +1 | +1 | -1 |
| 9 | -1 | -1 | -1 | +1 |
| 10 | +1 | -1 | -1 | +1 |
| 11 | -1 | +1 | -1 | +1 |
| 12 | +1 | +1 | -1 | +1 |
| 13 | -1 | -1 | +1 | +1 |
| 14 | +1 | -1 | +1 | +1 |
| 15 | -1 | +1 | +1 | +1 |
| 16 | +1 | +1 | +1 | +1 |

453
454

455 Table 2. Results of linearity: linear regression coefficient and p-value of the Student’s t-test on slope=0

| <div>Mapping system Sensor</div> | A | B | C | D |
|--|-------------------------------|-------------------------------|-------------------------------|-------------------------------|
| 1 | $R^2 = 0.978$ $p = 4.7e-6$ | $R^2 = 0.962$ $p = 8.8e-6$ | $R^2 = 0.982$ $p = 2.6e-8$ | $R^2 = 0.967$ $p = 2.1e-5$ |
| 2 | $R^2 = 0.961$ $p = 8.1e-5$ | $R^2 = 0.954$ $p = 1.0e-4$ | $R^2 = 0.936$ $p = 2.3e-4$ | $R^2 = 0.967$ $p = 2.5e-5$ |
| 3 | $R^2 = 0.972$ $p = 4.3e-7$ | $R^2 = 0.951$ $p = 3.9e-5$ | $R^2 = 0.964$ $p = 3.5e-7$ | $R^2 = 0.862$ $p = 9.0e-4$ |

456

Table 3. Results of linearity: Dispersion and standard deviation for sensors with the best and the worst linearity.

| Sensors | Applied pressure (mmHg) | Dispersion (mmHg) | Standard deviation |
|--|-------------------------|-------------------|--------------------|
| With the best linearity: sensor 1, mapping system C | 6.4 | 0 | 0 |
| | 13 | 1.74 | 0.641 |
| | 26 | 3.32 | 2.35 |
| | 39 | 2.97 | 1.54 |
| | 53 | 3.99 | 1.97 |
| | 79 | 9.05 | 3.22 |
| | 96 | 15.6 | 6.30 |
| With the worst linearity: sensor 3, mapping system C | 6.4 | 0 | 0 |
| | 13 | 0.103 | 0.0201 |
| | 26 | 0.120 | 0.0320 |
| | 39 | 1.01 | 0.376 |
| | 53 | 1.74 | 0.775 |
| | 79 | 4.35 | 1.97 |
| | 96 | 5.52 | 3.08 |

461 Table 4: Results of hysteresis: test in only one sensor per mapping system

| Mapping system | A | | | | | | | | B | | | | | | | |
|-------------------|------|------|------|------|------|------|------|------|------|------|------|-------|------|------|------|------|
| Sensor | 1 | 2 | 3 | 4 | 5 | 6 | 7 | 8 | 1 | 2 | 3 | 4 | 5 | 6 | 7 | 8 |
| Hysteresis Eh (%) | 15.2 | 16.9 | 7.63 | 4.58 | 11.9 | 7.84 | 16.1 | 10.1 | 3.51 | 6.38 | 11.7 | 0.228 | 18.3 | 15.7 | 27.9 | 9.20 |
| Mapping system | C | | | | | | | | D | | | | | | | |
| Sensor | 1 | 2 | 3 | 4 | 5 | 6 | 7 | 8 | 1 | 2 | 3 | 4 | 5 | 6 | 7 | 8 |
| Hysteresis Eh (%) | 3.99 | 4.53 | 7.13 | 2.80 | 5.26 | 3.15 | 9.93 | 2.70 | 6.52 | 3.15 | 3.66 | 3.63 | 2.27 | 3.99 | 10.5 | 7.20 |

462

463

464 Table 5. Results of hysteresis: test in all sensors per mapping system

| Mapping system | A | B | C | D |
|-------------------|------|------|------|------|
| Hysteresis Eh (%) | 9.41 | 7.87 | 7.58 | 6.29 |

465

466

Table 6. Results of the design of experiments for reproducibility. t: time, o: operators, l: location, w: weight

| Polynomial coefficient | Value | Probability |
|------------------------|-------|-------------|
| β_0 | 67.76 | 0 |
| β_t | 0.28 | 0.70 |
| β_o | 1.47 | 0.054 |
| β_l | 2.08 | 0.0080 |
| β_w | 19.19 | 0 |
| β_{to} | 1.94 | 0.0013 |
| β_{tl} | -3.84 | 0 |
| β_{tw} | -0.17 | 0.82 |
| β_{ol} | 0.66 | 0.38 |
| β_{ow} | 1.24 | 0.10 |
| β_{tw} | -0.73 | 0.33 |

Table 7. Results of surface condition: p_value of the statistical test to determine the statistically significant differences between measured pressure with and without fabric between the pressure mapping system and the table.

| Fabric | 1 | 2 | 3 | 4 | 5 |
|--------|---------------|---------------|---------------|---------------|---------------|
| | $2.97e^{-21}$ | $3.36e^{-18}$ | $3.77e^{-47}$ | $2.48e^{-31}$ | $8.17e^{-57}$ |

475 Table 8. Results of surface condition: linear regression coefficient for the second and third surface
 476 condition tests

| Sensors | 1 | 2 | 5 | 7 |
|-------------------------------|------|------|------|------|
| Second surface condition test | 0.97 | 0.95 | 0.97 | 0.99 |
| Third surface condition test | 0.92 | 0.93 | 0.98 | 0.95 |

477

478 Table 9. Results of mapping system superposition: p_value of the statistical test to determine the
 479 statistically significant differences between mapping system “from above” and “from the bottom”

| Sensors | 1 | 2 | 3 |
|--|--------|-------|--------|
| Between mapping system A: “from above” and mapping system B: “from the bottom” | 0.010 | 0.43 | 0.038 |
| Between mapping system C: “from above” and mapping system D: “from the bottom” | 0.0041 | 0.015 | 0.0058 |

480

481 Table 10. Results of mapping system superposition: absolute differences between measured pressures
 482 with or without superposition for each pressure mapping system in mmHg

| Mapping system | A | B | C | D |
|----------------|------|------|------|------|
| Sensor 1 | 10.3 | 14.6 | 3.94 | 4.16 |
| Sensor 2 | 14.0 | 12.5 | 2.97 | 2.48 |
| Sensor 3 | 9.32 | 23.0 | 9.64 | 2.75 |

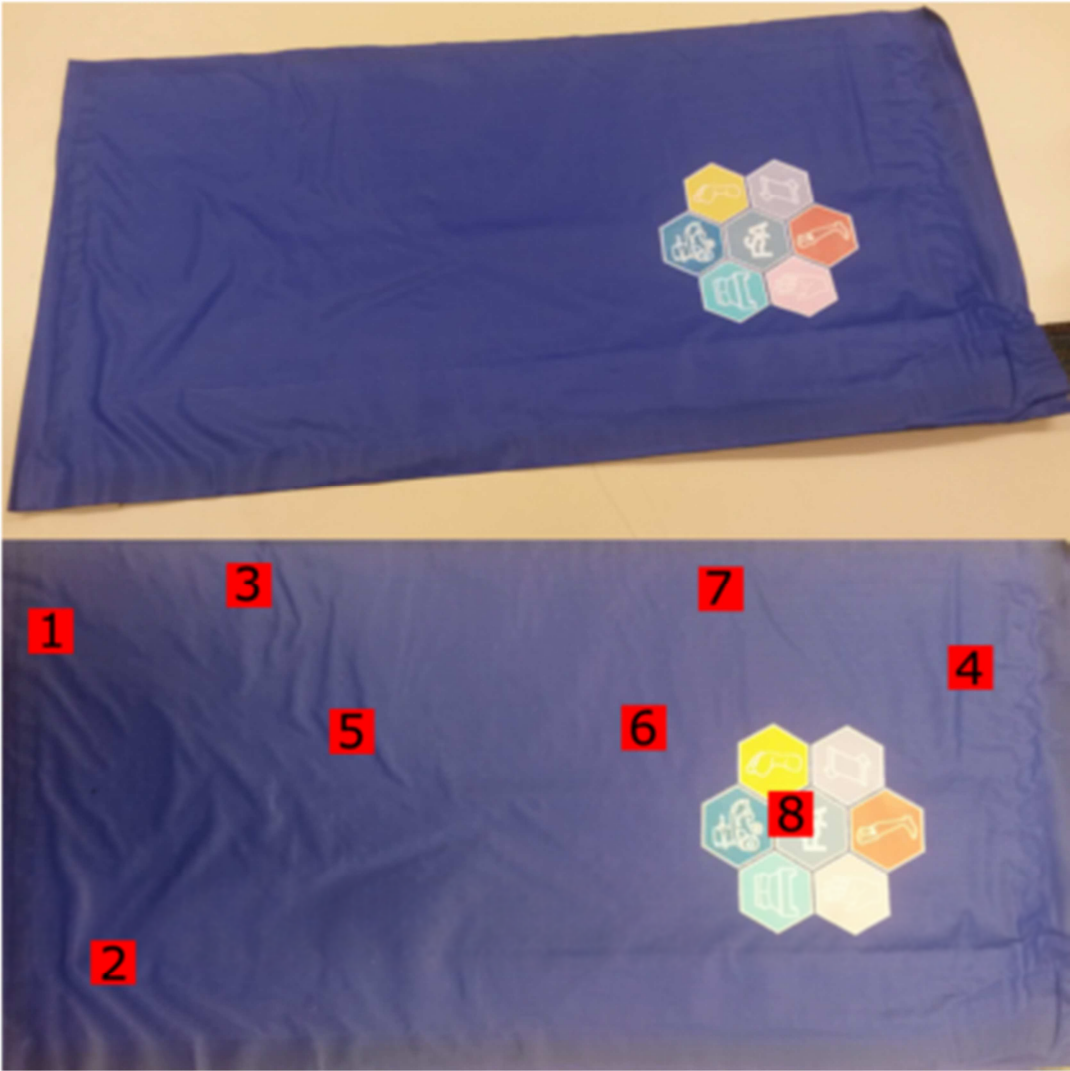
483
 484

485 Table 11. Comparison between the studied pressure mapping system and other commercial systems based
 486 on literature survey: resistive pressure mapping systems.

| Mapping system reference | FSA - | Tekscan's Flexiforce [22] | Tekscan's F- Socket [25] | Tekscan's F-Scan [21] | Rincoe [25] | Lück [29] |
|--------------------------------|-------------------|---------------------------------|--------------------------------|-----------------------------|----------------|--------------|
| Measurement error | 12.6 % | [5.62%, 26.3%] | 8.5±7.2% | 247% | 24.7±19.02% | -33% |
| Hysteresis | [6.29%, 9.41%] | 5.4±2.5% | 41.9±15% | - | 15.1±8% | - |

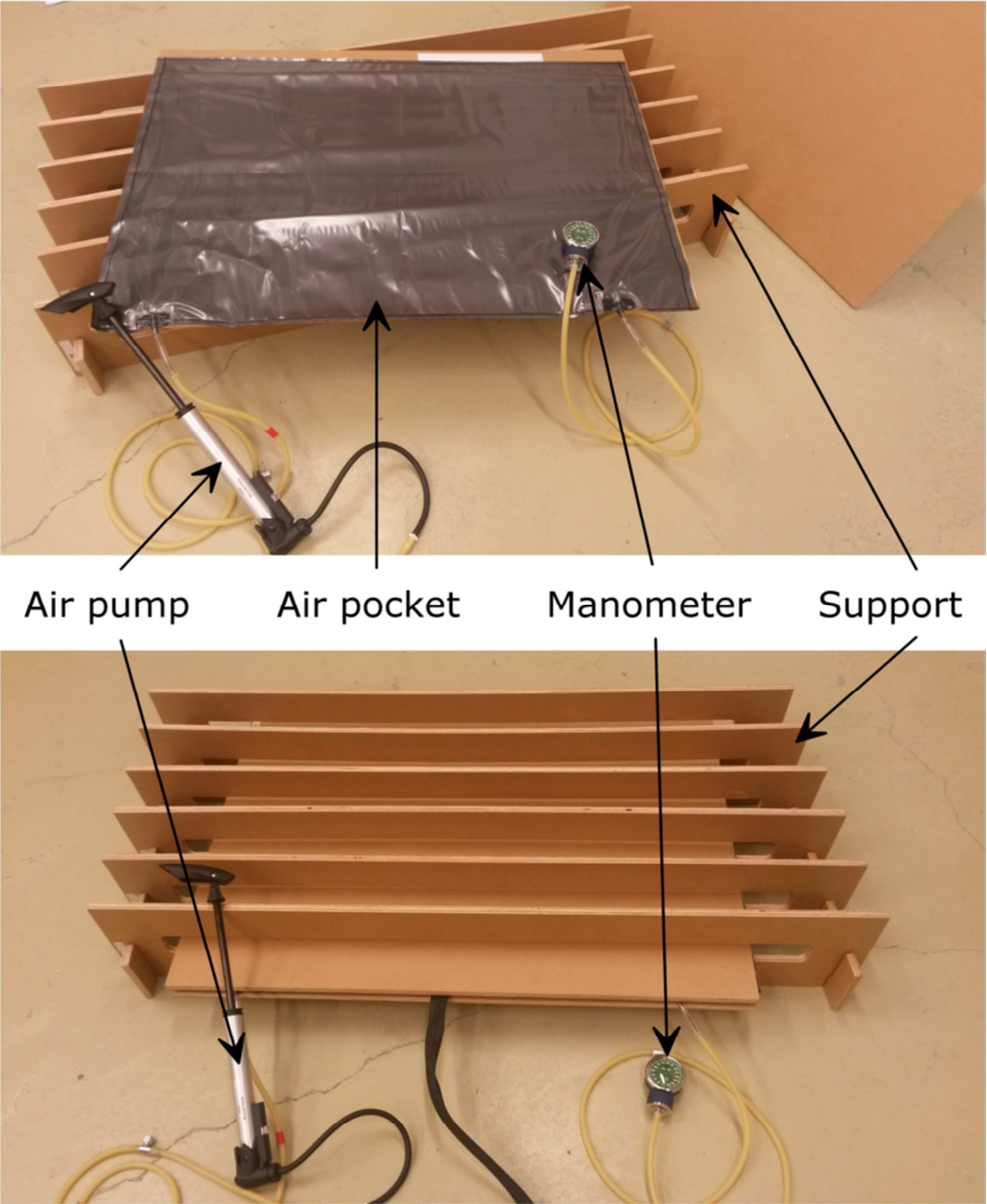
487

488 Figure 1. FSA Pressure mapping system

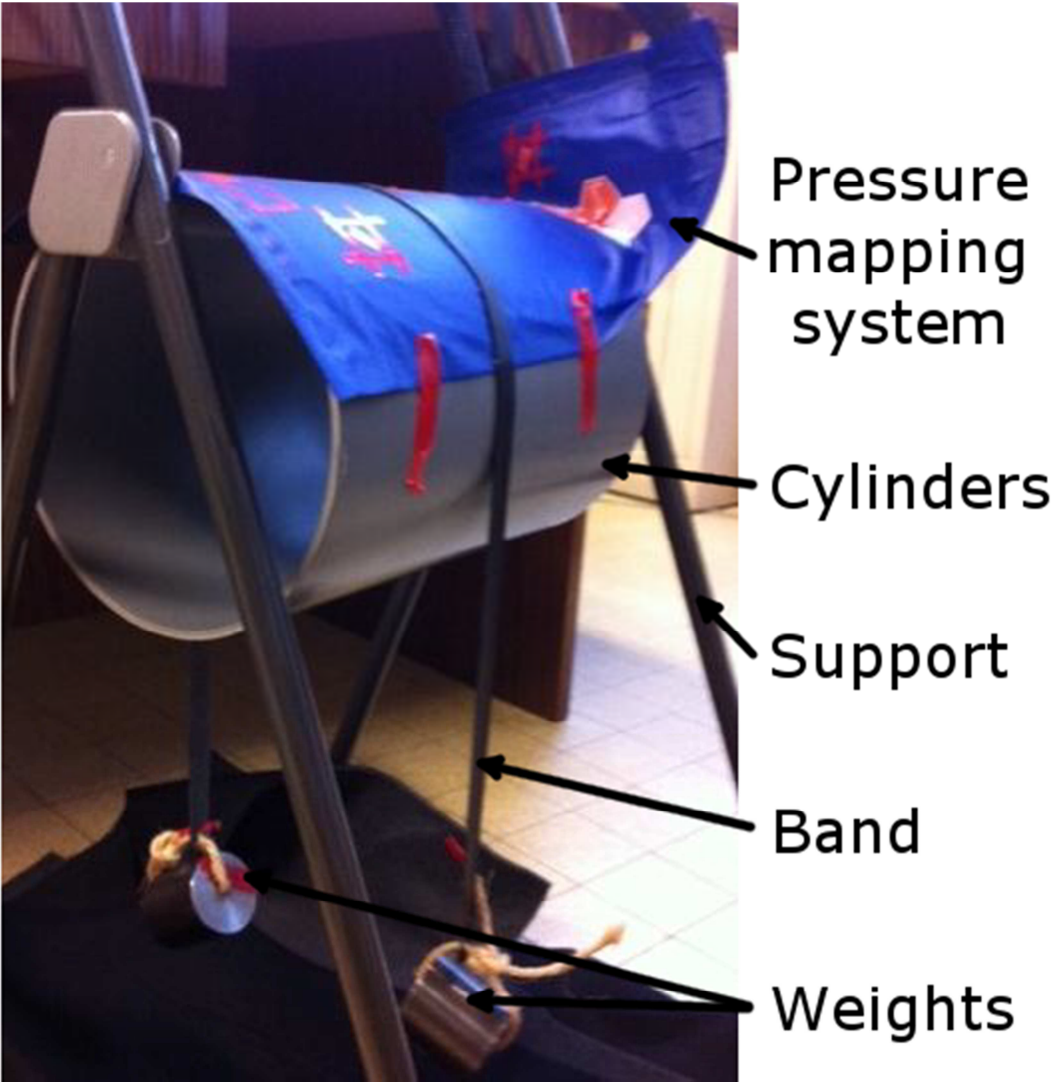


489

490 Figure 2. Experimental device for the second hysteresis test: (a) All elements of the experimental device,
491 (b) Device in used, with one pressure mapping system inside

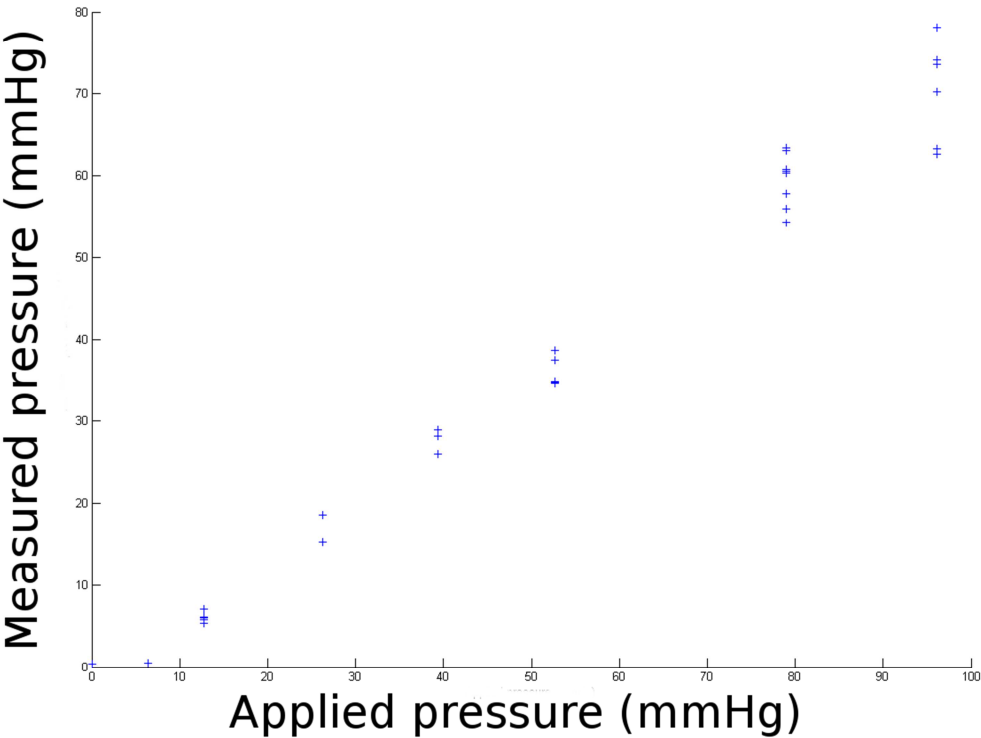


493 Figure 3. Experimental device for curvature test



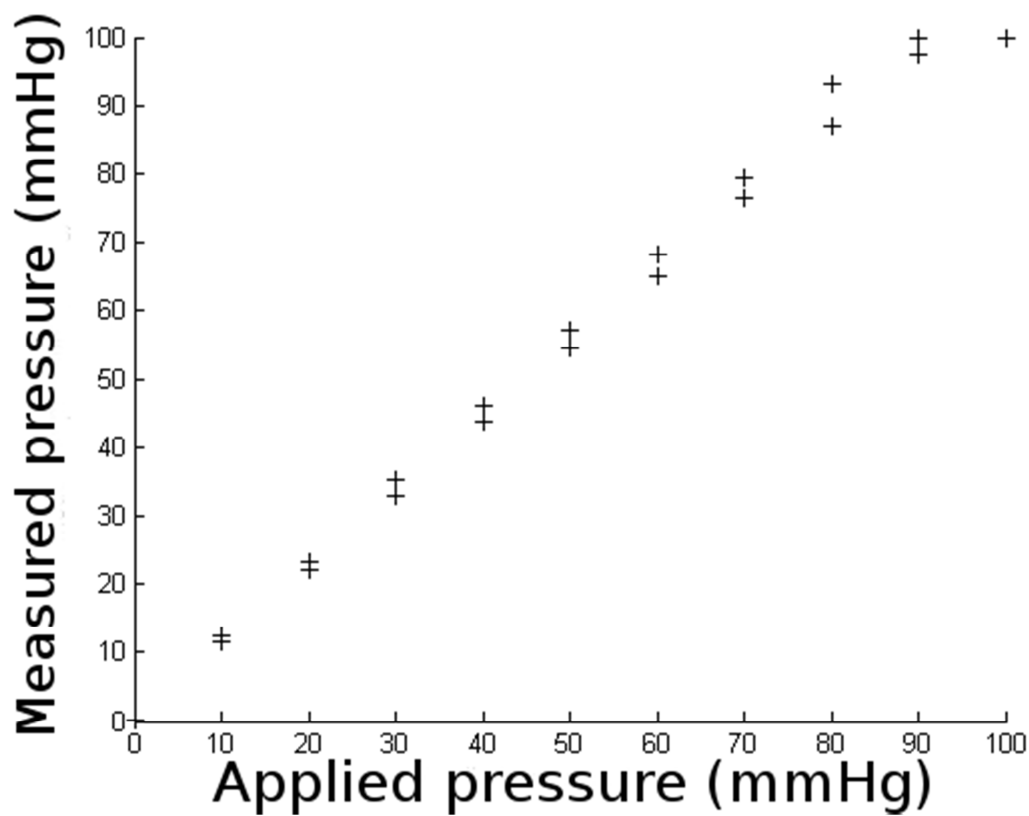
494

495 Figure 4. Results of linearity: measured pressure depending on applied pressure for the sensor 1 of the
496 pressure mapping system C



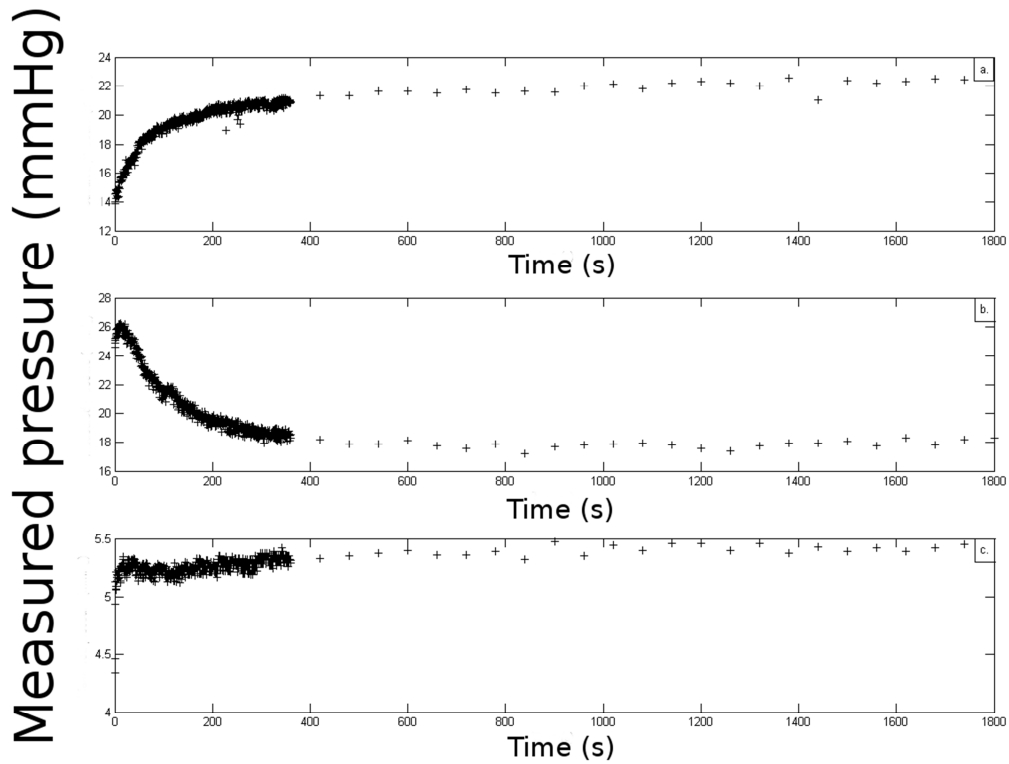
497

498 Figure 5: Results of the second hysteresis test (test in all sensors of a pressure mapping system): mean
499 measured pressure depending on applied pressure for mapping system A



500

501 Figure 6. Results of drift: (a) drift for 26mmHg applied pressure for mapping system A in the sensor 1,
502 (b) drift for 40mmHg applied pressure for mapping system C in the sensor 1, (c) drift for 26mmHg
503 applied pressure for mapping system D in the sensor 3



504

Figure 7. Results of curvature: normalized measured pressure depending on applied pressure and radius of cylinders Rc for mapping system A

